Journal of Materials Chemistry

Cite this: J. Mater. Chem., 2011, 21, 10384

www.rsc.org/materials

PAPER

Nanographite/polyaniline composite films as the counter electrodes for dye-sensitized solar cells†

Kuan-Chieh Huang,[a] Jen-Hsien Huang,[b] Chia-Hui Wu,[c] Chen-Yu Liu,[a] Hsin-Wei Chen,[a] Chih-Wei Chu,[bd] Jiann-T'suen Lin,[e] Cheng-Lan Lin*[f] and Kuo-Chuan Ho*[ac]

Received 8th February 2011, Accepted 9th March 2011
DOI: 10.1039/c1jm10576k

Nanographite/polyaniline (NG/PANI) composite films were developed and characterized, and the performances of the dye-sensitized solar cells (DSSCs) employing these composite films as the counter electrode (CE) were evaluated in this study. The nanographite/aniline (NG/ANI) particle was firstly synthesized by a reflux method and served as the monomer for the electro-polymerization of the NG/PANI composite films. The surface modification of NG by ANI was confirmed by EDX mapping, TEM image, zeta-potential, and UV-Vis absorption measurements. The electro-polymerized NG/PANI composite films were characterized by Raman spectroscopy, XPS, and conducting-AFM, which verified the successful incorporation of NGs in the PANI films. The electro-catalytic activity of the NG/PANI composite film was evaluated using the positive-feedback mode of scanning electrochemical microscopy (SECM), by which a comparable heterogeneous rate constant (k_s^0) for the ferrocene/ferrocenium (Fc/Fc^+) redox pair was obtained and compared with that of a sputtered Pt. The DSSC employing the NG/PANI (20 mC cm^{-2}) CE exhibited a higher short-circuit current density (J_{SC}) but lower fill factor (FF), and gave a comparable power-conversion efficiency (η) of 7.07%, as compared to that of a DSSC containing a sputtered Pt CE ($\eta = 7.19\%$).

1. Introduction

In a dye-sensitized solar cell (DSSC), the counter electrode (CE) is a crucial component for the accomplishment of an operating cycle.[1,2] Platinum (Pt) thin film coated transparent conductive oxides, such as indium-doped tin oxide (ITO) or fluorine-doped tin oxide (FTO), have been generally adopted as the CE in a DSSC because of their good electro-catalytic activity and high conductivity. Although Yen *et al.*[3] reported that the cost of Pt is only 0.02% in a DSSC, the basis for the calculation is not completely clear. Historically, the cost of precious materials varies significantly from time to time, especially when facing an energy crisis. Pt belongs to the energy material and is considered to be one of the most precious natural resources on earth. Thus, the feasibilities of using carbon-based materials or conducting polymers to replace Pt as the CE in a DSSC have been extensively investigated in recent years. For example, thin films of carbon-based materials such as carbon nanotube (CNT), graphite, and carbon black (CB)[4–15] have been employed as alternative CEs in DSSCs because of their good conductivities. Conducting polymers such as poly(3,4-ethylenedioxythiophene)–poly(styrene sulfonate) (PEDOT:PSS), poly(3,3-diethyl-3,4-dihydro-2*H*-thieno-[3,4-*b*][1,4]dioxepine) (PProDOT-ET_2), or polypyrrole have also been used.[16–20] Recently, environmentally stable polyaniline (PANI)[21–25] and the composites of PANI with carbon-based materials[26,27] have also been fabricated as the CEs in DSSCs. A partial list of literatures on the photovoltaic performances of DSSCs using various catalytic CEs based on carbon materials, conducting polymers, and carbon material/conducting polymer composites is summarized in Table 1.

The electro-catalytic activity and the conductivity of a non-Pt CE are the major factors deciding the performance of a DSSC employing such a CE. It is envisaged that a PANI film with well distributed nanographites (NGs) in it should be able to provide good conductivity as well as reasonable electro-catalytic activity for the use as a suitable CE in a DSSC. In this work, the nanographite/aniline (NG/ANI) particles were firstly synthesized, and the nanographite/polyaniline (NG/PANI) composite films were then electro-polymerized from the aqueous solutions containing such NG/ANI particles. The surface modification of NG by ANI

[a]*Department of Chemical Engineering, National Taiwan University, Taipei, 10617, Taiwan*
[b]*Research Center for Applied Sciences, Academia Sinica, Taipei, 11529, Taiwan*
[c]*Institute of Polymer Science and Engineering, National Taiwan University, Taipei, 10617, Taiwan. E-mail: kcho@ntu.edu.tw; Fax: +886-2-2362-3040; Tel: +886-2-2366-0739*
[d]*Department of Photonics, National Chiao Tung University, Hsinchu, 300, Taiwan*
[e]*Institute of Chemistry, Academia Sinica, Taipei, 11529, Taiwan*
[f]*Department of Chemical and Materials Engineering, Tamkang University, Tamsui Dist., New Taipei City, 25137, Taiwan. E-mail: cllin@mail.tku.edu.tw; Fax: +886-2-2620-9887; Tel: +886-2-2621-5656 ext. 2723*
† Electronic supplementary information (ESI) available. See DOI: 10.1039/c1jm10576k

Table 1 A partial list of literatures on the photovoltaic performances of DSSCs using various catalytic CEs based on carbon materials, conducting polymers, and carbon material/conducting polymer composites, at 100 mW cm^{-2} illumination

Catalysts on CEs	CE-substrates	TiO_2 area/cm^2	η (%)	Ref.
Single-wall CNT	FTO/glass	0.25	4.50	4
Multi-wall CNT	FTO/glass	0.36	7.59	6
Grafted multi-wall CNT	FTO/glass	—	7.03	7
Graphene	FTO/glass	0.39	5.00	12
Ordered multimodal porous carbon	FTO/glass	—	8.67	13
Ordered mesoporous carbon	FTO/glass	—	7.46	14
Acetylene black/graphite	FTO/glass	—	2.15	15
Polypyrrole	FTO/glass	—	7.66	16
PEDOT	ITO/PEN	—	8.00	17
PProDOT-Et_2	ITO/PEN	0.24	5.20	19
PANI	FTO/glass	—	4.95	21
PANI	FTO/glass	0.15	5.60	22
PANI	FTO/glass	—	7.15	24
Sulfamic acid-doped PANI	FTO/glass	0.25	5.50	25
Carbon black/PANI	FTO/glass	0.24	3.48	27
Nanographite/PANI	ITO/glass	0.16	7.07	This work

was examined by energy dispersive X-ray (EDX), transmission electron microscopy (TEM), zeta-potential, and UV-Vis absorption measurements. Raman spectroscopy and X-ray photoelectron spectroscopy (XPS) analyses were conducted to verify the incorporation of NGs in the PANI films. The conductivities and electro-catalytic activities of the NG/PANI composite films were estimated by the conducting atomic force microscopy (c-AFM) and the scanning electrochemical microscopy (SECM)[28–32] techniques. Finally, the performances of the DSSCs employing the NG/PANI composite films as the CEs were fabricated and evaluated.

2. Experimental

2.1. Materials

Nanographites (NGs, diameter ≈ 30 nm) were obtained from Ketjen Black Int. Company (Tokyo, Japan). Aniline (ANI), anhydrous LiI, I_2, acetonitrile (AN) and poly(ethylene glycol) (PEG, $M_w = 20\,000$) were purchased from Merck. Hydrochloric acid (HCl, 37%) and nitric acid (HNO_3, 65%) were obtained from Sigma-Aldrich. Ferrocene (Fc, 98%), titanium(IV) isopropoxide (TTIP, +98%), 4-*tert*-butylpyridine (TBP, 96%), and *tert*-butanol (TBA, 99.5%) were acquired from Acros. 3-Methoxypropionitrile (MPN, 99%) was obtained from Fluka. *cis*-Bis(isothio-cyanato) bis(2,2′-bipyridyl-4,4′-dicarboxylato)ruthenium(II)bis-tetrabutylammonium (N719) and 1,2-dimethyl-3-propylimidazolium iodide (DMPII) were purchased from Solaronix S. A., Aubonne, Switzerland.

2.2. Preparation of nanographite/polyaniline (NG/PANI) counter electrode

The ANI medium, containing different amounts (0.1, 0.2, 0.5, 1.0, and 1.5 wt%) of NGs, was refluxed at 210 °C for 3 h to prepare the NG/ANI particles. The NG/PANI composite films were then electro-polymerized from aqueous solution containing 1.0 M NG/ANI particles and 2.0 M HCl onto ITO (surface resistance = 10 Ω sq^{-1}, Uni-Onward Corp., Taipei, Taiwan) substrates using a constant potential of 0.8 V (*vs.* Ag/AgCl). The electro-polymerization was stopped when the desired amount of charge was passed. The as-prepared NG/PANI composite films were rinsed with hydrochloric solution, dried under air and served as the CEs in DSSCs.

2.3. Preparation of TiO_2 nanocrystalline film and fabrication of DSSC

The mesoporous TiO_2 nanocrystalline films were synthesized according to the procedures reported previously.[33] In brief, 72 mL of TTIP was added to an aqueous solution of 0.1 M HNO_3, and was vigorously stirred at 88 °C for 8 h. The resulting solution was then treated by a hydrothermal route in an autoclave at 240 °C for 12 h to obtain the aqueous mixture of nanocrystalline TiO_2. The mixture was concentrated to 13 wt% TiO_2, and 30 wt% of PEG (correspond to the TiO_2 content) was added. The obtained slurry was then doctor-bladed onto a FTO (surface resistance = 7 Ω sq^{-1}, TEC-7, Hartford Glass Co., Inc., Hartford City, Indiana, USA) substrate followed by annealing at 450 °C in air for 30 min. After repeating the above coating and annealing processes twice, a light scattering layer consisting of 300 nm TiO_2 particles was then coated on top of it and annealed at 450 °C in air for 30 min. The obtained mesoporous TiO_2 nanocrystalline film (project area = 0.16 cm^2) was immersed in an AN/TBA (v/v = 1/1) solution containing 0.3 mM N719 dye for 12 h. The dye-adsorbed TiO_2 photoanode was assembled with a CE, and a thermal plastics spacer (Surlyn® 1702, 25 μm thickness, Solaronix S. A., Aubonne, Switzerland) was used to seal the electrodes and control the distance between the two electrodes. The liquid electrolyte was a MPN solution containing 0.6 M DMPII, 0.1 M LiI, 0.05 M I_2, and 0.5 M TBP. The electrolyte was injected into the space separated by the thermal plastics spacer through capillary effect. The Pt thin film CE was sputter-deposited onto an ITO substrate using a Cressington 108 auto sputter coater (Cressington Scientific Instruments Ltd., Watford, UK), controlling at 40 mA and 130 s.

2.4. Instrumentation

The identification of various elements in the NG/ANI particles was carried out by the EDX equipped with a field-emission scanning electronic microscopy (FE-SEM, Zeiss EM 902A). The TEM image of the NG/ANI particles was observed by a JOEL JEM-1230 electron microscopy. The zeta potentials of the NG/ANI particles were measured by a 90Plus/BI-MAS particle sizing and zeta potential system (Brookhaven Instruments Corporation). The pH values of the NG/ANI particles were obtained by a pH meter (Orion 3 Star Benchtop, Thermo Electron Corporation). UV-Vis absorption spectra of the samples were measured by an UV/VIS/NIR spectrophotometer (V-570, Jasco). The Raman spectra were recorded by a Dimension-P2 Raman system (Lamba Solution, Inc.). XPS were performed with a PHI 5000 VersaProbe system (ULVAC-PHI, Chigasaki, Japan) using a microfocused (100 μm, 25 W) Al X-ray beam with a photoelectron takeoff angle of 45°. The Ar^+ ion source (FIG-5CE) was controlled by using a floating voltage of 0.2 kV. A Wienfiltered

C_{60}^+ ion source (IOG C60-10, Ionoptika, Chandler's Ford, UK) was operated at 10 mA and 10 kV. A c-AFM (E-sweep, Nano-Navi, SII Nanotechnology, Inc., Tokyo, Japan) equipped with a tapping mode micro-cantilever (SI-DF3-A, driving frequency, f = 24 kHz; spring constant, C = 1.1 N m^{-1}) that is coated with gold was employed to estimate the surface conductivities of the films. The DSSCs were illuminated by a class A quality solar simulator (PEC-L11, AM 1.5G, Peccell Technologies, Inc.), and the incident light intensity (100 mW cm^{-2}) is calibrated with a standard silicon cell (PECSI01, Peccell Technologies, Inc.). The photoelectrochemical characteristics of the DSSCs were recorded with a potentiostat/galvanostat (PGSTAT 30, Autolab, Eco-Chemie, the Netherlands). A CHI model 900B SECM (CH Instruments, Austin, TX) was employed to carry out the electrochemical experiments.

2.5. Electrochemical and SECM experiments

A Pt ultramicroelectrode (UME, 10 μm in diameter, the ratio between the insulator thickness and the radius of the microdisk electrode, RG = 3), a Pt wire, and a Ag/Ag$^+$ electrode were employed as the working electrode, the auxiliary electrode, and the reference electrode, respectively. The electrolyte was AN solution containing 50 mM $LiClO_4$ and 1.0 mM ferrocene (Fc). All potentials reported are referred to the Ag/Ag$^+$ reference electrode. The linear sweep voltammetry (LSV) curve was obtained by scanning the potential of a Pt UME from −0.3 to 0.5 V with a scan rate of 20 mV s^{-1}. For the SECM experiments, a Pt UME (tip), which carried out the electro-oxidation of ferrocene (Fc) to ferrocenium (Fc$^+$) at 0.5 V, was moved toward the substrate (at 0.08 V) with a constant velocity of 5 μm s^{-1}. As the tip–substrate distance, d, became smaller than the thickness of the diffusion layer, the tip-generated Fc$^+$ was reduced to Fc by the substrate and then diffused back to the tip, which causes an increase in the anodic current response of the tip. Such "positive-feedback approaching curves" were recorded and were employed to estimate the heterogeneous rate constants (k_s^0) of the reaction at different substrates.

3. Results and discussion

3.1. Preparation of aniline (ANI) modified nanographite (NG)

The main purpose of this study is to develop a NG/PANI composite film modified ITO electrode as the CE for a DSSC. At first, the NG/ANI particles were prepared by incorporating NGs into an ANI medium and followed by continuous stirring at 210 °C for 3 h. The obtained NG/ANI particles were then analyzed by EDX mapping for identifying the major components of the composites, as shown in Fig. 1. The carbon and nitrogen elements were detected and observed in the selected square zones of Fig. 1a and b, respectively. Thus, it is noticed that the nitrogen belongs to the ANI, which attach to the surfaces of NGs. In addition, Fig. 2a shows the TEM image of the NG/ANI particles dispersed in an aqueous solution. The zeta-potentials, ξ, for the NGs and the NG/ANI particles in aqueous solutions were measured to be −35.08 ± 2.40 mV (pH 6.59 ± 0.05) and −43.61 ± 0.74 mV (pH 6.71 ± 0.04), respectively, which provide a further verification for the surface modification of the NGs (Fig. 2b). It has been reported that nanocomposites with a larger

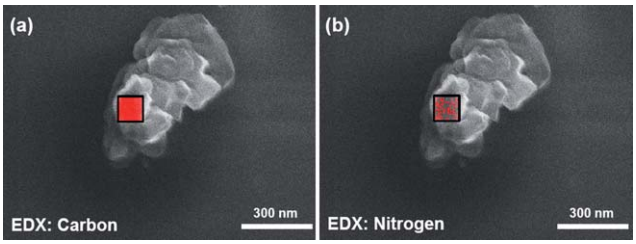

Fig. 1 EDX mapping images of NG/ANI particles for identification of (a) carbon and (b) nitrogen.

|ξ| value have better dispersion ability in aqueous solutions.[34] A larger |ξ| value for the NG/ANI particles than that of the NGs implies better dispersion ability for the NG/ANI particles in an aqueous solution. UV-Vis absorption spectra of the NG/ANI particles and the pristine ANI measured in aqueous solutions are also exhibited in Fig. 2c. The characteristic absorption peak of ANI centered at around 280 nm appears for the NG/ANI particles. This implies the existence of the ANI on the surfaces of NGs. The above-mentioned EDX mapping, TEM images, ξ-potential, and UV-Vis absorption analyses suggest the successful modification of the NGs surface by ANI.

3.2. Characterization of NG/PANI composite films

The NG/PANI composite films were prepared by electro-polymerizing from an aqueous solution containing the NG/ANI particles, which served as monomers, onto ITO substrates at various charge capacities. The resulted NG/PANI composite films were examined by Raman spectroscopy (Fig. 3). The characteristic peaks at around 1340 and 1598 cm^{-1} correspond to

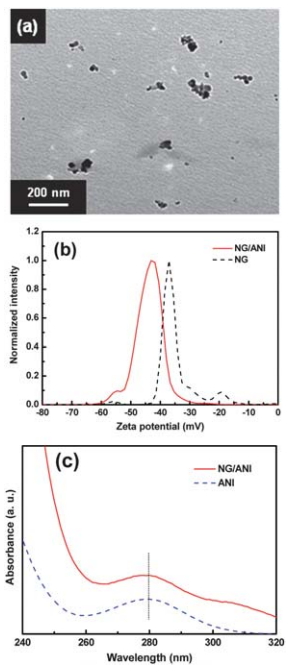

Fig. 2 (a) TEM image and (b) zeta-potential spectra of NG/ANI particles and NGs. (c) UV-Vis absorption spectra of the NG/ANI particles and the pristine ANI in aqueous solutions.

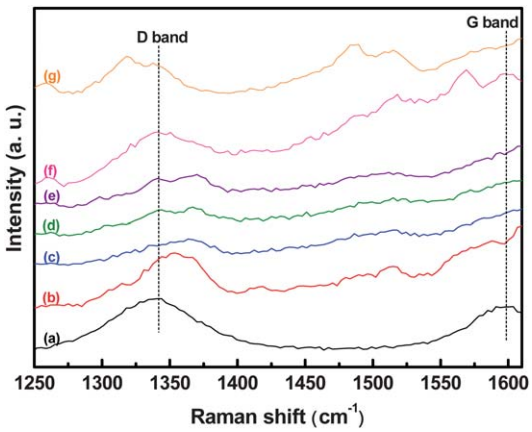

Fig. 3 Raman spectra of (a) NGs, (b) pristine PANI (20 mC cm^{-2}), and the NG/PANI composite films which were electro-polymerized (20 mC cm^{-2}) from aqueous solutions with (c) 0.1, (d) 0.2, (e) 0.5, (f) 1.0, and (g) 1.5 wt% of NGs in NG/ANI particles.

the D and G band of the NG, respectively. The relative intensity of the D band (1340 cm^{-1}) of the NG/PANI composite films increased as the amount of NGs in the NG/ANI particles increased from 0.2 to 1.0 wt% during the electro-polymerization process. In addition, the relative intensity of the G band (1598 cm^{-1}) of the NG/PANI composite film can be observed at 1.0 wt% of NGs in the NG/ANI particles employed during the electro-polymerization. The above results confirm the incorporation of the NG/ANI particles inside the electro-polymerized PANI films. However, the relative intensities for both D and G bands decreased as the amount of NGs in the NG/ANI particles reached 1.5 wt%. This implies the higher amount (1.5 wt%) of NGs may be not totally electro-polymerized onto the ITO. Thus, the optimal amount of 1.0 wt% of NGs in the NG/PANI composite films was chosen for the following studies.

The XPS spectra for both the PANI and the NG/PANI composite films are shown in Fig. 4. The chemical analysis of the films is characterized by the XPS with a mixture of Ar^+ and C_{60}^+ ions gun. The chemical states for the films are preserved while a steady co-sputtering rate is achieved and the probing depth increases. The binding energy of the C–C bonding, within both NG and PANI, is at around 283.5 eV. The XPS intensity of PANI and NG/PANI composite films is about the same before sputtering (Fig. 4a). As the sputtered time increased to 10 and 20 min, the peak at 283.5 eV for the NG/PANI composite films rendered higher intensity (Fig. 4b and c). These observations implied the existence of NGs inside the PANI, which is consistent with the Raman spectroscopy results mentioned earlier.

The c-AFM technique is utilized to investigate the surface conductivity of the NG/PANI composite film. The NG/PANI composite film prepared from the solution containing 1.0 wt% NGs in the NG/ANI particles was chosen for c-AFM characterization because it exhibits explicit D band enhancement in Raman spectra. The c-AFM images for both the NG/PANI composite film and the PANI film at an applied potential of −0.4 V are shown in Fig. 5a and b, respectively. The surface of the NG/PANI composite film possesses more uniform current distribution and has a higher average current, as compared to that of a pristine PANI, suggesting that the NGs were better

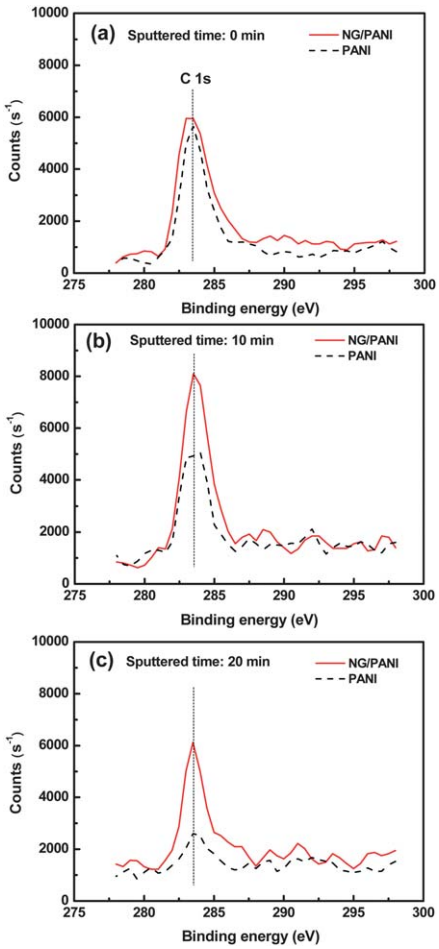

Fig. 4 XPS spectra of NG/PANI (20 mC cm^{-2}) composite and pristine PANI (20 mC cm^{-2}) films obtained with sputtered time of (a) 0, (b) 10, and (c) 20 min.

distributed over the surface of the NG/PANI composite film and contributed to larger surface conductivity.

3.3. Analysis of electro-catalytic abilities for the CEs by SECM

To gain an insight into the electro-catalytic ability of the NG/PANI composite films, the heterogeneous rate constants, k_s^0, of the Fc/Fc^+ redox reaction at the NG/PANI modified electrode surfaces were investigated by the positive feedback mode of the SECM technique. The behavior of a positive-feedback approaching curve depends on k_s^0 of the substrate reaction as well as the potential applied to the substrate. A dimensionless reaction kinetic factor Λ is defined as ak_s^0/D_{app}, where a is the radius of the Pt UME and D_{app} is the apparent diffusion coefficient of Fc.[35] The D_{app} of Fc was estimated to be 2.17×10^{-5} $cm^2\ s^{-1}$ using the equation $i_{ss} = 4nFCaD_{app}$, where i_{ss} is the steady current response of the tip at infinite distance away from the substrate, n is number of electrons involved in the reaction, F is Faradic constant, and C is bulk concentration of the Fc.[36] The formal potential for the Fc/Fc^+ redox pair (acquired from a LSV experiment, not shown here, using a Pt UME) is 0.08 V, which is chosen as the potential applied to the substrate during the experiments.

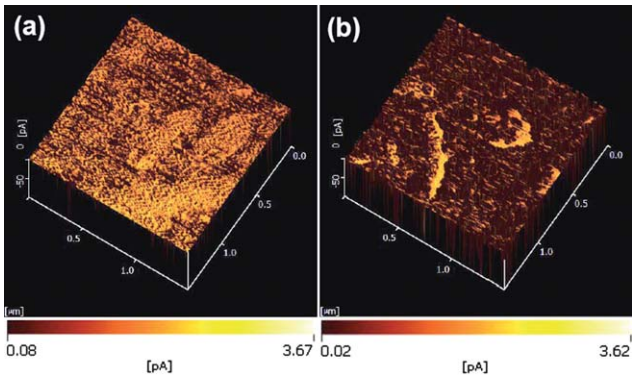

Fig. 5 C-AFM images of (a) the NG/PANI (20 mC cm^{-2}) composite film and (b) a pristine PANI (20 mC cm^{-2}) film at an applied potential of −0.4 V.

Fig. 6 shows the theoretical positive-feedback approaching curves for $\Lambda = 1$ and 5 when the substrate's applied potential was 0.08 V. The ordinate is the normalized tip current, i_T ($= i_{tip}/i_{ss}$), and the abscissa is the normalized distance, L ($= d/a$). The tip current responses with a NG/PANI composite film and a sputtered Pt film as the substrates fit the positive-feedback approaching curve for $\Lambda = 5$, which corresponds to a k_s^0 value of ~0.217 cm s^{-1}. The value of k_s^0 for a pristine PANI film substrate was estimated to be ~0.043 cm s^{-1} using the same method. The results indicate that the incorporation of NGs into a pristine PANI film enhanced its electrochemical performance, and the NG/PANI composite film exhibits comparable electro-catalytic ability with that of a Pt film. The presence of uniformly distributed NGs within the PANI matrices is responsible for the high electro-catalytic ability of the composite film achieved.

3.4. Photovoltaic performances of DSSCs assembled with various CEs

The photocurrent–voltage (I–V) characteristics of DSSCs fabricated using NG/PANI CEs with different charges of electropolymerization are presented in Fig. 7. All photovoltaic parameters are summarized in Table 2. The short-circuit current densities (J_{SC}) and power-conversion efficiencies (η) of the DSSCs with NG/PANI CEs were higher than the DSSC with a pristine PANI CE. Such performance enhancement is attributed to the presence of NGs, incorporated uniformly inside the NG/PANI composite film, which provides higher conductivity. The enhancement is also due to both NGs and PANI of the NG/PANI composite film's own electro-catalytic abilities at the same time for facilitating the I_3^- reduction in the electrolyte. When the DSSC employed the CE of NG/PANI composite film with a charge capacity of 10 mC cm^{-2}, the J_{SC} for this DSSC was 19.39 mA cm^{-2}, which was lower than that of the DSSC containing the CE of NG/PANI with a charge capacity of 20 mC cm^{-2} (J_{SC} = 20.14 mA cm^{-2}). This indicates a NG/PANI composite film (20 mC cm^{-2}) provides larger active surface areas for the I_3^- reduction. Nevertheless, the J_{SC} decreases to 16.96 mA cm^{-2} for the DSSCs based on a 60 mC cm^{-2} NG/PANI CE. When the electropolymerizing charge capacity is controlled at greater than 20 mC cm^{-2} (Fig. 7), the decrease in J_{SC} may be attributed to the increase in the internal series resistance of the composite film. For comparison, the DSSC fabricated using a bare NG CE delivered J_{SC} of 6.80 mA cm^{-2} and an efficiency of 3.11%, as shown in Fig. S1 (ESI†).

The DSSC assembled with a sputtered Pt CE showed the highest fill factor (FF) among all DSSCs. This is due to the lower interfacial resistance between the Pt CE and the electrolyte accomplished by the dense and compact surface morphology of the Pt film. The DSSCs employing a pristine PANI or NG/PANI CEs all achieved higher J_{SC} than the DSSC fabricated using a Pt CE. This might be attributed to the PANI-based film having a porous structure, which provides larger active surface areas for the I_3^- reduction. Both NGs and pristine PANI can be employed as the catalysts on CEs because of their fair conductivities and catalytic abilities toward I_3^- reduction (Fig. S1† and Fig. 7). The NG/PANI composite film, prepared at the optimal condition (1.0 wt% NG, 20 mC cm^{-2}) in this study, significantly improved the charge-transfer ability within this composite network, which is evident in the higher J_{SC} observed for the DSSC assembled with this NG/PANI CE. The higher J_{SC} and lower FF obtained

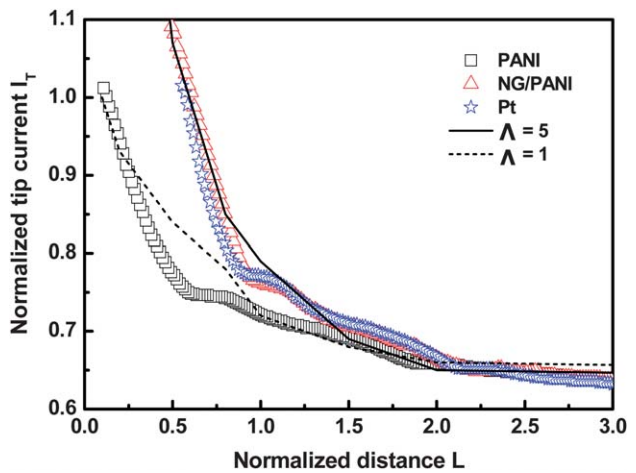

Fig. 6 Normalized positive feedback approaching curves for pristine PANI (20 mC cm^{-2}), NG/PANI (20 mC cm^{-2}), sputtered Pt substrates, and the theoretical curves for Λ of 5 and 1.

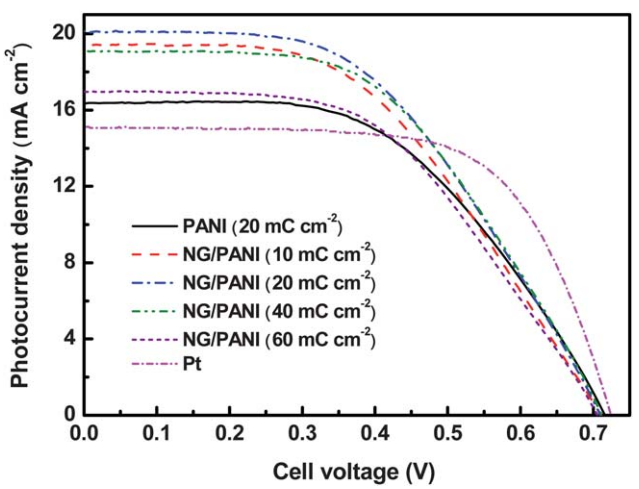

Fig. 7 I–V characteristics of DSSCs fabricated using different CEs. The DSSCs are illuminated at 100 mW cm^{-2} light intensity.

Table 2 Photovoltaic parameters of DSSCs fabricated with CEs consisting of pristine PANI (20 mC cm^{-2}), 1.0 wt% of NGs in the NG/PANI composite films, which were electro-polymerized at charge capacities of 10, 20, 40, and 60 mC cm^{-2}, and sputtered Pt (incident light intensity: 100 mW cm^{-2})

CEs	V_{OC}/V	FF	J_{SC}/mA cm^{-2}	η (%)
PANI (20 mC cm^{-2})	0.72	0.52	16.34	6.16
NG/PANI (10 mC cm^{-2})	0.71	0.49	19.39	6.74
NG/PANI (20 mC cm^{-2})	0.71	0.49	20.14	7.07
NG/PANI (40 mC cm^{-2})	0.71	0.52	19.11	7.00
NG/PANI (60 mC cm^{-2})	0.71	0.51	16.96	6.16
Pt	0.72	0.66	15.13	7.19

for a DSSC with a pristine PANI CE than those for a DSSC with a Pt-based CE were reported by Zhang *et al.*[21] Although the DSSC assembled with a NG/PANI (20 mC cm^{-2}) CE had a lower FF, but it achieved a higher J_{SC}, which resulted in a comparable performance at 100 mW cm^{-2} illumination, with reference to a DSSC using a Pt CE.

4. Conclusions

The NG/PANI composite films were successfully electro-polymerized onto ITO electrodes from the aqueous solution containing various amounts of NG/ANI particles as the monomers. The EDX mapping, TEM image, ζ-potential, and UV-Vis absorption measurements confirmed the formation of NG/ANI particles by the incorporation of NGs in an ANI medium through a reflux process. The NG/PANI composite films derived from the NG/ANI particles exhibited more uniform and higher surface conductivity, compared to that of a pristine PANI film, and such improvement has to do with the well-distributed NGs in the PANI matrices. The positive-feedback mode of the SECM experiments also suggested that the NG/PANI (20 mC cm^{-2}) composite film exhibited a comparable electro-catalytic ability toward the Fc/Fc^{+} redox reaction, as compared to that of a sputtered Pt film. The *I–V* characteristics of the DSSCs fabricated using the NG/PANI composite films with different NG loadings as the CEs were evaluated. It was found that higher J_{SC} and lower FF were achieved for the DSSCs with the NG/PANI composite films, as compared to those of the DSSC with a sputtered Pt CE. It is deduced that the lower FF obtained is due to the higher interfacial resistance between the NG/PANI composite film and the electrolyte. Further studies on the factors causing the enhancement in J_{SC} are in progress. The DSSC employing the NG/PANI (20 mC cm^{-2}) CE achieved a power-conversion efficiency (η) of 7.07%, which is comparable to that of a DSSC with a Pt CE ($\eta = 7.19\%$). The above results suggested that the NG/PANI composite can serve as a potential alternative material for the replacement of conventional Pt CE in a DSSC.

Acknowledgements

This work was financially supported by the National Science Council and the Academia Sinica of Taiwan.

References

1 B. O'Regan and M. Grätzel, *Nature*, 1991, **353**, 737.
2 N. Papageorgiou, *Coord. Chem. Rev.*, 2004, **248**, 1421.
3 M. Y. Yen, C. Y. Yen, S. H. Liao, M. C. Hsiao, C. C. Weng, Y. F. Lin, C. C. M. Ma, M. C. Tsai, A. Su, K. K. Ho and P. L. Liu, *Compos. Sci. Technol.*, 2009, **69**, 2193.
4 K. Suzuki, M. Yamaguchi, M. Kumagai and S. Yanagida, *Chem. Lett.*, 2003, 28.
5 W. J. Lee, E. Ramasamy, D. Y. Lee and J. S. Song, *ACS Appl. Mater. Interfaces*, 2009, **1**, 1145.
6 E. Ramasamy, W. J. Lee, D. Y. Lee and J. S. Song, *Electrochem. Commun.*, 2008, **10**, 1087.
7 J. Han, H. Kim, D. Y. Kim, S. M. Jo and S. Y. Jang, *ACS Nano*, 2010, **4**, 3503.
8 S. I. Cha, B. K. Koo, S. H. Seo and D. Y. Lee, *J. Mater. Chem.*, 2010, **20**, 659.
9 A. Kay and M. Grätzel, *Sol. Energy Mater. Sol. Cells*, 1996, **44**, 99.
10 K. Imoto, K. Takahashi, T. Yamaguchi, T. Komura, J. I. Nakamura and K. Murata, *Sol. Energy Mater. Sol. Cells*, 2003, **79**, 459.
11 T. N. Murakami, S. Ito, Q. Wang, M. K. Nazeeruddin, T. Bessho, I. Cesar, P. Liska, R. H. Baker, P. Comte, P. Péchy and M. Grätzel, *J. Electrochem. Soc.*, 2006, **153**, A2255.
12 J. D. R. Mayhew, D. J. Bozym, C. Punckt and I. A. Aksay, *ACS Nano*, 2010, **4**, 6203.
13 S. Q. Fan, B. Fang, J. H. Kim, B. Jeong, C. Kim, J. S. Yu and J. Ko, *Langmuir*, 2010, **26**, 13644.
14 E. Ramasamy, J. Chun and J. Lee, *Carbon*, 2010, **48**, 4563.
15 T. Denaro, V. Baglio, M. Girolamo, V. Antonucci, A. S. Arico', F. Matteucci and R. Ornelas, *J. Appl. Electrochem.*, 2009, **39**, 2173.
16 J. Wu, Q. Li, L. Fan, Z. Lan, P. Li, J. Lin and S. Hao, *J. Power Sources*, 2008, **181**, 172.
17 J. M. Pringle, V. Armel and D. R. MacFarlane, *Chem. Commun.*, 2010, **46**, 5367.
18 S. Ahmad, J. H. Yum, Z. Xianxi, M. Grätzel, H. J. Butt and M. K. Nazeeruddin, *J. Mater. Chem.*, 2010, **20**, 1654.
19 K. M. Lee, C. Y. Hsu, P. Y. Chen, M. Ikegami, T. Miyasaka and K. C. Ho, *Phys. Chem. Chem. Phys.*, 2009, **11**, 3375.
20 A. Kanciurzewska, E. Dobruchowska, A. Baranzahi, E. Carlegrim, M. Fahlman and M. Girţu, *J. Optoelectron. Adv. Mater.*, 2007, **9**, 1052.
21 J. Zhang, T. Hreid, X. Li, W. Guo, L. Wang, X. Shi, H. Su and Z. Yuan, *Electrochim. Acta*, 2010, **55**, 3664.
22 Z. Li, B. Ye, X. Hu, X. Ma, X. Zhang and Y. Deng, *Electrochem. Commun.*, 2009, **11**, 1768.
23 Q. Qin, J. Tao and Y. Yang, *Synth. Met.*, 2010, **160**, 1167.
24 Q. H. Li, J. H. Wu, Q. W. Tang, Z. Lan, P. J. Li, J. M. Lin and L. Q. Fan, *Electrochem. Commun.*, 2008, **10**, 1299.
25 S. Ameen, M. S. Akhtar, Y. S. Kim, O. B. Yang and H. S. Shin, *J. Phys. Chem. C*, 2010, **114**, 4760.
26 H. Sun, Y. Luo, Y. Zhang, D. Li, Z. Yu, K. Li and Q. Meng, *J. Phys. Chem. C*, 2010, **114**, 11673.
27 N. Ikeda and T. Miyasaka, *Chem. Commun.*, 2006, 1733.
28 P. Sun, F. O. Laforge and M. V. Mirkin, *Phys. Chem. Chem. Phys.*, 2007, **9**, 802.
29 K. R. J. Lovelock, F. N. Cowling, A. W. Taylor, P. Licence and D. A. Walsh, *J. Phys. Chem. B*, 2010, **114**, 4442.
30 B. Bozic and E. Figgemeier, *Chem. Commun.*, 2006, 2268.
31 Y. Shen, K. Nonomura, D. Schlettwein, C. Zhao and G. Wittstock, *Chem.–Eur. J.*, 2006, **12**, 5832.
32 Y. Shen, U. M. Tefashe, K. Nonomura, T. Loewenstein, D. Schlettwein and G. Wittstock, *Electrochim. Acta*, 2009, **55**, 458.
33 J. G. Chen, V. Suryanarayanan, K. M. Lee and K. C. Ho, *Sol. Energy Mater. Sol. Cells*, 2007, **91**, 1432.
34 Z. Sun, V. Nicolosi, D. Rickard, S. D. Bergin, D. Aherne and J. N. Coleman, *J. Phys. Chem. C*, 2008, **112**, 10692.
35 M. V. Mirkin, in *Scanning Electrochemical Microscopy*, ed. A. J. Bard and M. V. Mirkin, Marcel Dekker, New York, 2001, ch. 6, pp. 201–219.
36 N. G. Tsierkezos, *J. Solution Chem.*, 2007, **36**, 289.